Title
Effects of bentonite heating on U(VI) adsorption

Authors
Fox, Patricia M
Tinnacher, Ruth M
Cheshire, Michael C
et al.

Publication Date
2019-10-01

DOI
10.1016/j.apgeochem.2019.104392

Effects of bentonite heating on U(VI) adsorption

Patricia M. Fox* [a], Ruth M. Tinnacher [a, b], Michael C. Cheshire [c, d], Florie Caporuscio [c], Sergio Carrero [a ,e], and Peter S. Nico [a]

*corresponding author: pmfox@lbl.gov

[a] Earth & Environmental Sciences Area, Lawrence Berkeley National Laboratory, 1 Cyclotron Road, Berkeley, CA 94720

[b] Department of Chemistry & Biochemistry, California State University East Bay, Hayward, CA 94542

[c] Earth and Environmental Sciences, Los Alamos National Laboratory, MS J966, Los Alamos, NM 87545

[d] current address: Oak Ridge National Laboratory, 1 Bethel Valley Road, Oak Ridge, TN, 37831

[e] Department of Earth and Planetary Science, University of California Berkeley, McCone Hall, Berkeley, CA 94720-4767

Submitted to Applied Geochemistry

Revised version submitted July 2019

Graphical Abstract

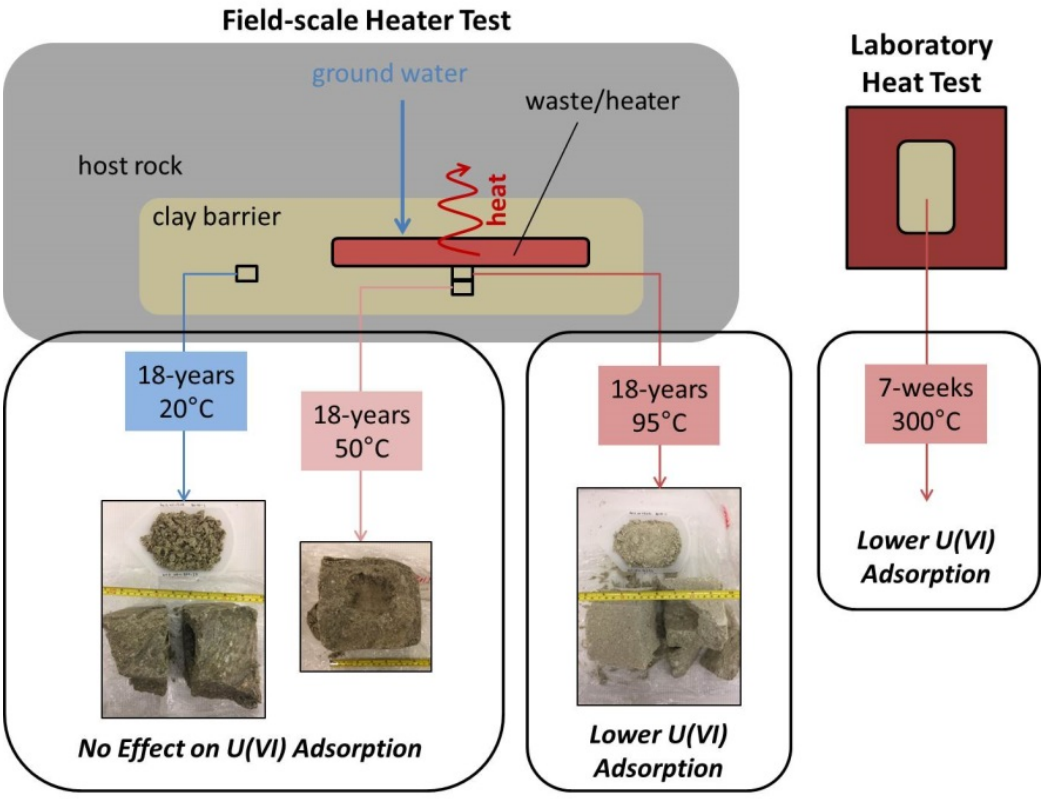

Highlights

- Uranium adsorption onto field-heated (95°C, 18-years) and lab-heated (300°C, 7-weeks) bentonite was lower than onto control samples over a range of chemical conditions.
- Intermediate-heated bentonite (50°C, 18-years) showed no change in U(VI) adsorption compared to control samples.
- On average, K_d values decreased by 31% for field-heated bentonite and 50% for lab-heated bentonite.
- Lower U adsorption persisted on field-heated samples after purification and isolation of the clay fraction.
- No evidence of illitization was observed after heating; we propose that heat-induced changes to clay may be limited to edge site effects under these conditions.

Keywords

Uranium; adsorption; bentonite; nuclear waste disposal; radioactive waste; FEBEX; engineered barriers

Abstract

Engineered barrier systems designed to isolate high-level radioactive waste utilize bentonite, a montmorillonite-rich material, to restrict contaminant transport due to its low hydraulic conductivity and high adsorption capacity. High temperatures (100-200°C) near waste canisters resulting from radioactive decay may alter the clay's ability to adsorb contaminants. In this study, we examine U(VI) adsorption onto two different bentonite samples subjected to (1) 18 years of *in situ* heating during an underground experiment and (2) short-term (7-week), high temperature (300°C) heating in the laboratory. Results show that U(VI) adsorption was lower for field-heated bentonite located closest to the heater, which experienced temperatures of approximately 95°C, compared to a control sample, which experienced temperatures of approximately 20°C, over a range of aqueous chemical conditions. On average, K_d values for U(VI) adsorption were 31% lower for 95°C heated samples. By contrast, U(VI) adsorption onto intermediate-heated bentonite (50°C) was indistinguishable from the adsorption onto the cold-zone (20°C) sample. U(VI) adsorption onto lab-heated bentonite was also lower than onto control bentonite over the pH range 4.5-8.0, with an average decrease in K_d values of 50% after heating. Lower U(VI) adsorption to field-heated bentonite persisted after bentonite was purified to isolate the clay fraction. This allows us to rule out changes in pore-water chemistry or accessory mineral composition as causes of the lower adsorption. No evidence of montmorillonite illitization was observed in the heated samples. While some of the lower U(VI) adsorption in the lab-heated bentonite can be explained by changes in aqueous U(VI) speciation, we propose that lower U(VI) adsorption to field-heated bentonite may be primarily due to changes in the montmorillonite edge structure. The observed changes in U(VI) adsorption to

bentonite after heating have implications for U(VI) diffusive transport through engineered barriers and must be considered when designing radioactive waste disposal repositories.

1. Introduction

Uranium (U) contamination in the subsurface is a part of the legacy of nuclear weapons and energy production, resulting from mining and milling activities, processing of nuclear materials, and used nuclear fuel disposal. The U.S. Department of Energy (DOE) is tasked with cleaning up U-contaminated aquifers at a number of sites, including the Uranium Mill Tailings Remedial Action (UMTRA) sites and the Savannah River, Oak Ridge, and Hanford sites where a variety of different radionuclides are present. In order for nuclear energy to be viable, a long-term nuclear waste disposal repository capable of isolating high-level (HLW) and low-level radioactive waste (LLW) over the time scales necessary for the decay of long-lived radioactive isotopes (> 10^6 years) must be created. Most disposal options currently under investigation use clay media (*i.e.*, bentonite or shale) as engineered barriers or as the host rock for geologic storage (Altmann, 2008; Altmann et al., 2012; Delay et al., 2007; Guyonnet et al., 2009; SKB, 2011; Tournassat et al., 2015). Clays are good barriers for HLW due to their low hydraulic conductivity, which restricts contaminant mobility to slow diffusion-based transport, and their high adsorption capacity for radionuclides, which slows transport even further. Montmorillonite ($M^{+}_{0.33}(Al_{1.67}Mg_{0.33})Si_4O_{10}(OH)_2$) is the dominant clay mineral found in bentonite. It has a 2:1 layer-type phyllosilicate structure, with a large specific surface area (~750 m^2/g) and cation exchange capacity (~1 mol_c/kg), and strongly-sorbing surface complexation sites on clay edge surfaces.

Uranium can exist in both the tetravalent and hexavalent oxidation state, however, due to the limited solubility of U(IV), U(VI) is the most common oxidation state found in the dissolved phase. U(VI) adsorption varies as a function of pH, bicarbonate, and Ca^{2+} concentrations due to changes in U(VI) aqueous speciation (Fox et al., 2012; Fox et al., 2006; Stewart et al., 2010;

Tournassat et al., 2018). At moderate bicarbonate concentrations (> 1 mM) above pH 7, U(VI) speciation is dominated by uranyl-carbonato complexes [UO_2CO_3(aq), $UO_2(CO_3)_2^{2-}$, $UO_2(CO_3)_3^{4-}$] in the absence of Ca, and calcium-uranyl-carbonato ternary complexes [$Ca_2UO_2(CO_3)_3$(aq), $CaUO_2(CO_3)_3^{2-}$] in the presence of typical groundwater Ca concentrations (> 1 mM) (Dong and Brooks, 2006; Fox et al., 2006; Guillaumont et al., 2003). These calcium-uranyl-carbonato complexes adsorb weakly or not at all to mineral surfaces, and thus changes in U(VI) speciation have a large impact on its sorption and transport behavior (Fox et al., 2012; Fox et al., 2006; Stewart et al., 2010).

Storage of HLW can result in transient high temperatures near the waste canisters resulting from radioactive decay. The effects of elevated temperature on the engineered barrier must be taken into account when designing a nuclear waste repository. The duration of the transient elevated temperature and temperature profiles in the engineered barrier can vary widely depending on the repository design and site-specific (*e.g.*, host rock) factors, however most HLW repository concepts impose a temperature limit of 100-200°C in the bentonite buffer, with elevated temperatures persisting for on the order of thousands of years (Johnson et al., 2002; Wersin et al., 2007; Zheng et al., 2015). Temperature effects on the bentonite barrier may include changes to the clay's hydrological and mechanical properties, changes to pore water chemical compositions, and changes to the clay and accessory mineral composition (Cuadros and Linares, 1996; Wersin et al., 2007; Zheng et al., 2015). The conversion of montmorillonite to illite, known as illitization, is one of the primary mineralogical changes expected to occur during long-term exposure to high temperatures. Zheng et al. (2015) predicted the extent of illitization over a 1000 year simulation to be 1-8% (volume fraction) at 100°C, and 1-27% at 200°C in a modeling study. Concentrations of pore water potassium (K) and the abundance and dissolution rate of K-

feldspar were the primary chemical factors controlling the extent of illitization in their study (Zheng et al., 2015). Cementation of clay particles, *e.g.*, through precipitation of SiO_2 particles, leading to a loss of swelling capacity may also occur as a result of bentonite heating, particularly under unsaturated conditions (Couture, 1985; Pusch et al., 2003; Wersin et al., 2007). Intrusion of groundwater from the surrounding host rock may also have an effect on clay properties. In order to investigate these combined effects on an engineered barrier, the FEBEX (Full-Scale Engineered Barriers Experiment) *in situ* heater test was conducted by Empresa Nacional de Residuos Radiactivos (ENRESA) under the auspices of the European Union at the Grimsel Test Site from 1997 to 2015 (Villar et al., 2018a; Villar et al., 2018b). Highly compacted bentonite blocks, serving as the engineered test barrier, were placed in a radial arrangement around two underground heaters and heated to a maximum of 100°C in a crystalline host rock (ENRESA, 2000).

The goal of this work was to study U(VI) adsorption behavior on bentonite heated under realistic field conditions compared to laboratory-heated bentonite. Aqueous U(VI) speciation calculations and mineralogical characterization are used to aid in the interpretation of the results. This study provides useful information for a waste disposal scenario in which leaking of the waste canister begins after the transient thermal perturbation has passed.

2. Materials and Methods

2.1 Bentonite Samples

Two types of bentonite samples were used for the experiments to test the effect of heating: (1) laboratory-heated and control (un-heated) bentonite, and (2) bentonite from the heater-zone and cold-zone of a long-term field-scale experiment. Bentonite for the laboratory heated samples was mined from a reducing horizon in Colony, Wyoming, and contains 72% Na-montmorillonite

136 with minor amounts of clinoptilolite, feldspars, biotite, cristobalite, quartz and pyrite (Cheshire et
137 al., 2014). The bentonite, known as sample EBS-12 (Caporuscio et al., 2014; Caporuscio et al.,
138 2013), was mixed with an artificial groundwater solution (Table 1) at a solid-liquid ratio of 5:1
139 by weight and exposed to a temperature of 300°C and a pressure of 150-160 bar for 7 weeks as
140 described in detail by Cheshire et al. (2014). Both the heat-treated and starting material (control)
141 were pulverized with a Retsch MM 400 ball mill (frequency of 30/sec for 2 minutes) prior to
142 U(VI) sorption experiments.

143 Long-term heated and cold-zone bentonite samples were obtained from the second dismantling
144 of the FEBEX *in situ* heater test in 2015, after 18 years of heating. Detailed information on the
145 FEBEX test can be found elsewhere (Detzner and Kober, 2015; ENRESA, 2000). The original
146 FEBEX bentonite was mined from the Cortijo de Archidona deposit (Almería, SE Spain) and
147 contained primarily expandable clays (92%), with minor amounts of quartz (2%), plagioclase
148 (2%), cristobalite (2%), and traces of potassium feldspar, calcite, and tridymite (Fernández et al.,
149 2004). The expandable clays are primarily illite-smectite mixed layered material with
150 approximately 11% of illitic layers (Fernández et al., 2004). Briefly, bentonite was compacted
151 into blocks at 1650 kg/m^3 dry density, placed in a radial arrangement around two underground
152 heaters and heated to a maximum of 100°C. Kinetic experiments were used to screen bentonite
153 samples for differences in U(VI) adsorption (see details in SI) and three locations were selected
154 for further study: two locations in the heater test zone (BD-48) at radial distances of 50-cm
155 (closest to heater) and 75-cm from the center axis and one location from a control non-heated
156 zone (BD-59) at 50-cm. Three replicate blocks from each location were split open and bentonite
157 was removed from the center of each block. Bentonite samples were dried at 60°C for 1 week,
158 crushed by hand using a porcelain mortar and pestle, and sieved through a 0.063 mm sieve in

order to remove sand particles and reduce sample heterogeneity. Equivalent weights of each replicate block were mixed together to form composite samples for the three locations. Average water contents of bulk FEBEX samples determined immediately after dismantling were approximately 18%, 24%, and 25% and historical *in situ* temperatures were approximately 95°C, 50°C, and 20°C for the 50-cm heater-zone, 75-cm heater-zone, and 50-cm cold-zone samples, respectively (Villar et al., 2018a; Villar et al., 2018b).

Table 1. Artificial groundwater chemistry used during heat treatment of laboratory-heated bentonite. Data from Caporuscio et al. (2014).

Species	Concentration (mg/L)
Ca	43
Cl	686
K	299
Na	162
Si	2
SO4	31
Sr	<0.05
TDS[(a)]	1226
pH	6.93

[(a)] TDS = total dissolved solids

2.2 Bentonite Extraction and Purification

171 Composite FEBEX bentonite samples were extracted and purified in order to compare
172 extractable metal concentrations between the samples and produce a purified clay sample for
173 U(VI) adsorption experiments. The extraction and purification procedure was adapted from
174 Tinnacher et al. (2016) to allow for an additional characterization of extracted metals. The
175 procedure included the following major steps: (1) leaching of clay samples with water, (2)
176 leaching with, and dialysis against, sodium acetate at pH 5 for carbonate mineral removal, (3)
177 dialysis against NaCl to remove acetate and complete Na-saturation, (4) dialysis against water to
178 remove excess salts, and (5) centrifugation to remove particles greater than 2 μm. Detailed
179 methods are presented in the SI. Solution samples from leaching with water (step 1) were
180 analyzed for water soluble metals, dissolved inorganic carbon (DIC), and pH, and acetate
181 leachates (step 2) were analyzed for metals. Laboratory-heated and control bentonite samples
182 were treated in a similar manner for characterization purposes, but were not completely purified
183 (*i.e.*, only steps 1 and 2 were performed). All reported extraction data represent the average and
184 standard deviation of triplicate extractions.

185 ***2.3 Batch Adsorption Experiments***

186 Batch equilibrium U(VI) adsorption experiments were conducted on un-purified ("bulk")
187 laboratory heated and control bentonite and on purified and un-purified ("bulk") FEBEX
188 bentonite composite samples over a range of chemical compositions at room temperature.
189 Laboratory heated bentonite experiments were conducted over the pH range of 4 to 9 in 0.1 M
190 NaCl background electrolyte, buffered with $NaHCO_3$ for pH values greater than 6.5. The FEBEX
191 bentonite experiments were conducted at two Ca concentrations over a pH range of 7 to 8 at an
192 ionic strength of 0.1 M, using NaCl as the background electrolyte. We did not test pH values
193 greater than 8 for the FEBEX bentonite experiments due to supersaturation with respect to calcite

194 (at 2 mM Ca) and low U(VI) adsorption at alkaline pH. Solid concentrations for all experiments
195 were 0.5 g/L and total initial U(VI) concentrations were approximately 1 x 10^{-6} M. For purified
196 FEBEX clay samples, two separate experiments were conducted with Ca added to yield
197 concentrations of 0.1 and 2.0 mM in solution, respectively. The 0.1 mM Ca concentration was
198 chosen based on the concentrations of Ca released from unpurified bentonite samples. In
199 unpurified FEBEX bentonite samples, some Ca was present in the clay, so two samples were
200 prepared, spiked with zero or 2.0 mM Ca, achieving final dissolved Ca concentrations of
201 approximately 0.1 and 2.1 mM, respectively.

202 Adsorption experiments were conducted in 40-mL polycarbonate centrifuge tubes. Clay
203 samples were suspended in DI water (diluted from 10 g/L stock suspension) and aliquots of 1 M
204 NaCl, 0.1 M $CaCl_2$, and 0.1 M $NaHCO_3$ stock solutions were added to reach the desired final
205 concentrations and to facilitate equilibration with atmospheric CO_2 for samples above pH 7. The
206 pH was then adjusted to target values using 0.1 M HCl or NaOH and samples were allowed to
207 equilibrate for 24 hours on an end-over-end sample rotator. After equilibration, samples were
208 spiked with U(VI) using a 3 x 10^{-4} M U(VI) stock, pH was re-adjusted, and samples were placed
209 again on an end-over-end rotator for 48 hours to allow for U(VI) adsorption. Samples were then
210 centrifuged at 39,000 x *g* for 20 minutes (or 15,000 x *g* for 60 minutes) and the supernatant was
211 collected for analysis by ICP-MS (U, Ca, and other metals), DIC, and pH. These centrifugation
212 conditions were sufficient to remove all particles >24 nm as calculated by Stoke's Law.
213 Adsorbed U(VI) is expressed as log K_d, where K_d is the amount of U(VI) adsorbed to the clay (in
214 mol/kg clay) divided by the final dissolved U(VI) concentration (in mol/L). Adsorbed U(VI)
215 concentrations are expressed in terms of the dry weight of clay (dried at 150°C).

216 ***2.4 Analytical Techniques***

DIC was measured on a Shimadzu TOC-V analyzer. Samples were analyzed for metal concentrations by ICP-MS (Perkin-Elmer Elan DRC II) after acidification and dilution with ultrapure (ultrex grade) 0.15 M nitric acid and internal standard addition.

Analytical electron microscopy was performed on laboratory heated and control bentonite using a FEI™ Inspect F scanning electron microscope (SEM). All samples were Au/Pd-coated prior to SEM analysis. Imaging with the SEM was performed using a 5.0 kV accelerating voltage and 1.5 spot size. Energy dispersive X-ray spectroscopy (EDX) was performed at 30 kV and a 3.0 spot size.

The mineralogical composition of both bentonite samples were analyzed using XRD (Chung, 1974). The <2 μm particles were separated in DI water. Purified FEBEX bentonite was dispersed with 1 mM sodium pyrophosphate addition. An aliquot of the <2 μm suspension was dropped on a zero-background plate and dried at room temperature. Each FEBEX sample was measured (3 to 25/75°2θ at 2 to 10 s per step with Cu Kα) under four different conditions: (1) dry at room temperature, (2) saturated with ethylene-glycol for 1 hour at 60°C, (3) heated at 400°C for 1 hour, and (4) heated at 550°C for 1 hour. The laboratory bentonite was analyzed (2 to 40 °2θ at 8 to 12 s per step with Cu Kα) under two different conditions: (1) dry at room temperature and (2) saturated with ethylene glycol for 24 hours at 60°C. Illite abundance within the illite/smectite for the FEBEX bentonite were calculated using the method described by Drits et al. (1994). Illite abundances in illite/smectite for the laboratory bentonites were calculated via the Δ°2Θ method (Eberl et al., 1993; Moore and Reynolds, 1989; Srodon, 1980).

2.5 Cation Exchange Capacity

Cation exchange capacity was measured using the hexamine cobalt method according to Hadi et al. (2013). Triplicate samples of 50 mg dry clay were weighed into centrifuge tubes and 10 mL

of 15 mM hexamine cobalt(III) chloride solution was added. Samples were mixed on an end-over-end sample rotator for 2 hours, then centrifuged at 39,000 x *g*. Control water extract samples were prepared in the same manner using 50 mg of clay and 10 mL of MilliQ water. Solution samples were analyzed for major cations (Ca, Mg, K, and Na) by ICP-MS and the cation exchange capacity was calculated from the sum of cations released from the hexamine cobalt solution corrected for any soluble salts released during the water extracts. CEC is expressed as $mmol_c/g$ (mmol of charge per gram dry clay). Calculations from the sum of cations method agreed with results calculated from the loss of absorbance at 475 nm. However, because the precision was better for the sum of cation method, only the results from this method are presented.

2.6 U(VI) Aqueous Speciation Calculations

Thermodynamic calculations were performed in order to determine aqueous U(VI) speciation during batch adsorption experiments using Visual Minteq version 3.1. The standard Visual Minteq database was used, which uses data for U species from the NEA database (Guillaumont et al., 2003), the THERMOCHIMIE database (Giffaut et al., 2014), and Dong and Brooks (2006). Data for other species are from the NIST database (Smith et al., 2003). The final measured values for pH, DIC, Ca, Mg, K, and total U(VI) were used along with an assumed NaCl concentration of 0.1 M for speciation calculations. The partial pressure of CO_2 (pCO_2) was calculated, and varied between 300 and 620 ppm for FEBEX experiments, values that are reasonable given that experiments were performed under atmospheric conditions (approximate CO_2 of 380 ppm) in closed vessels. Calculated pCO_2 was more variable for laboratory bentonite (heated and control) experiments (237-2,094 ppm), which will be discussed in section 3.3.

Aqueous U(VI) speciation diagrams only show species with contributions >0.1% to the total U(VI) concentration (*i.e.*, 10^{-9} M).

2.7 U(VI) Diffusion Calculations

In order to demonstrate the potential impacts of heat-induced alterations on U(VI) diffusion through an engineered barrier we performed diffusion calculations using an analytical solution to Fick's law (Shackelford, 1991). Equation 1 describes diffusion of a solute through porous media from a single source solution of constant concentration into an infinite clay (*i.e.*, non-steady state conditions) (Shackelford, 1991):

$$\frac{c}{c_0} = erfc\left(\frac{x}{2\sqrt{D^* t/R_d}}\right), \qquad \text{Equation 1}$$

where c is the concentration of the solute in the porewater solution, c_0 is the concentration of the solute in the source reservoir, *erfc* is the complementary error function, x is the distance from the source reservoir, D^* is the effective diffusion coefficient, t is time and R_d is the retardation factor. D^* describes the diffusion of solutes in porous media and is directly proportional to the diffusion coefficient of the solute in free water (D_0) according to Equation 2:

$$D^* = \tau D_0 \qquad \text{Equation 2}$$

where τ is tortuosity. Note that according to the convention of Shackelford (1991), D^* does not include porosity. R_d can also be expressed in terms of the K_d using Equation 3:

$$R_d = 1 + \left(\frac{\rho_d}{\varepsilon}\right) K_d\,, \qquad \text{Equation 3}$$

where ρ_d is the dry density and ε is the porosity. This approach assumes that adsorption is linear with respect to solute concentration. U(VI) adsorption onto montmorillonite has been shown to

be linear over a range of low U(VI) concentrations (*e.g.*, equilibrium concentration of 10^{-9} to 10^{-7} M at pH 6.8), with non-linear adsorption occurring at higher U(VI) concentrations (Bradbury and Baeyens, 2005; Marques Fernandes et al., 2012) making linearity a reasonable assumption. The K_d values obtained from our experiments on heated and cold-zone bulk FEBEX bentonite were then used along with the values listed in Table 2 to calculate concentrations of U(VI) in porewater as a function of time and distance from the source solution. García-Gutiérrez et al. (2003) estimated effective diffusion coefficient (D_e) values of 0.6-2.2 x 10^{-12} m^2/s for U(VI) diffusion through compacted FEBEX bentonite, where D_e is defined by Equation 4:

$$D_e = \varepsilon D^* \qquad \text{Equation 4.}$$

We used an average value of 1.4 x 10^{-12} m^2/s for D_e from García-Gutiérrez et al. (2003), which corresponds to 3.5 x 10^{-12} m^2/s for D^* for diffusion estimates. While K_d may vary as a function of distance from the heater due to temperature profile in the bentonite barrier, these calculations are intended to illustrate the maximum potential effect of bentonite heating on U(VI) transport.

Table 2. Input values used for U(VI) diffusion calculations.

Parameter	**Value**
c_0	1 x10^{-5} M
D^*	3.5 x 10^{-12} m^2/s [(a)]
ρ_d	1.65 kg/L
ε	0.4

[(a)] D^* calculated from García-Gutiérrez et al. (2003) for U(VI) diffusion through compacted FEBEX bentonite.

3. RESULTS AND DISCUSSION

3.1 Bentonite Characterization Results

Water extractions of unpurified FEBEX bentonite released greater concentrations of major cations (Na, K, Ca, and Mg) for the 95°C heated sample compared to the cold-zone sample (20°C) as shown in Table 3. Changes in aqueous porewater chemistry, particularly pH, DIC, and Ca concentration will lead to changes in aqueous U(VI) speciation and clay edge site protonation, thereby affecting adsorption (Tournassat et al., 2018). The heater-zone sample water leachates yielded lower DIC and pH values. Soluble ion concentrations in the *in situ* samples may be altered compared to the original material due to intrusion of groundwater and/or heat-induced alterations. For example, lower soluble metal concentrations in the cold-zone sample may represent either a metal loss due to groundwater leaching in this sample or a relative increase in metal concentrations in the heated sample. The latter may, for instance, be caused by the transport of salts from the surrounding bentonite and/or granite formation into the heated-zone, where they are deposited through evaporation. While we did not perform extractions on the original bentonite sample, Fernández et al. (2004) reported concentrations of soluble salts during leaching experiments with the original FEBEX bentonite, although at a slightly higher solid to liquid ratio (0.15 kg/L compared to 0.1 kg/L in our study). In general, salt concentrations observed in the leachates of the original bentonite were in between the values observed in our study for the 95°C-heated and 20°C cold zone samples (Na = 10.3 mM, K = 0.10, Mg = 0.12 mM, Ca = 0.10 mM), while pH (8.76) was closer to the pH in our cold-zone sample (Fernández et al., 2004). Villar et al.(Villar et al., 2017) reported similar results for water extracts of FEBEX samples performed at solid-liquid ratios of 1:2.5 and 1:4 as a function of radial distance from the heater. They observed an increase in Na, Ca, and Cl concentrations and in electrical conductivity

and a decrease in DIC and pH close to the heater compared to the original bentonite. The change in pH and DIC in particular is noteworthy, as it could suggest that carbonate minerals may have been depleted or altered in the heated sample. For example, a fraction of calcite may have been converted to a lower-solubility carbonate mineral as a result of heating. The pH 5 acetate extractions released slightly higher Mg and Ca concentrations in the 95°C heated sample compared to the cold-zone sample. The acetate extractions are designed to dissolve carbonate minerals such as calcite and dolomite, but can also release adsorbed cations.

The laboratory-heated bentonite had slightly higher Na and K, and lower Ca and Mg concentrations in the water extracts compared to the control sample, whereas the acetate extractions released slightly higher concentrations of K, Ca, and Mg for the lab-heated sample. Similar to the FEBEX samples, the lab-heated sample also had a slightly lower pH and DIC value than the control sample in water extracts. Changes in water soluble and acetate-extractable salt concentrations in the lab-heated sample may reflect changes in mineralogy and mineral solubility which occurred as a result of heating.

336 **Table 3**. Chemical characterization of bentonite samples by water and acetate extractions. Concentrations of extracted constituents are

337 expressed as the average and standard deviation of replicate extracts.

	pH	DIC (mM)	Na (mM)	K (mM)	Ca (mM)	Mg (mM)
	Water Extractions					
FEBEX 95°C heated	7.96 ± 0.02	1.02 ± 0.04	11.30 ± 0.13	0.192 ± 0.008	0.370 ± 0.004	0.356 ± 0.002
FEBEX 50°C heated	8.33 ± 0.03	1.55 ± 0.04	7.52 ± 0.09	0.074 ± 0.000	0.068 ± 0.005	0.050 ±0.000
FEBEX 20°C cold	8.63 ± 0.12	2.07 ± 0.04	7.69 ± 0.19	0.077 ± 0.000	0.069 ± 0.001	0.088 ± 0.002
lab heated	9.50 ± 0.06	4.41 ± 0.01	13.01 ± 0.14	0.058 ± 0.001	0.053 ± 0.004	0.130 ± 0.032
lab control	10.16 ± 0.02	5.31 ± 0.25	11.03 ± 0.37	0.017 ± 0.001	0.100 ± 0.006	0.556 ± 0.017
	Acetate Extractions					
FEBEX 95°C heated	NM*	NM	NM	1.37 ± 0.03	24.97 ± 0.57	16.83 ± 0.09
FEBEX 50°C heated	NM	NM	NM	1.25 ± 0.03	23.69 ± 0.39	14.30 ± 0.43
FEBEX 20°C cold	NM	NM	NM	1.34 ± 0.05	24.17 ± 0.18	15.28 ± 0.00
lab heated	NM	NM	NM	1.20 ± 0.11	5.96 ± 0.12	0.84 ± 0.00
lab control	NM	NM	NM	0.60 ± 0.02	4.69 ± 0.12	0.57 ± 0.02

338

339 *NM=not measured

Results from bulk XRD and SEM analysis of the laboratory bentonite before and after heat-treatments are shown in Table 4 and Figure 1. Some changes were observed in the accessory mineral fraction after heating, including lower fractions of clinoptilolite and biotite than the starting material. The formation of authigenic phases were observed after heating, including the formation of analcime at a fraction of 1% or greater and an increase in SiO_2 phases (cristobalite or opal-CT) from 2% to 10%. The increase in SiO_2 phases is consistent with previous observations of cementation of clay particles by SiO_2 during heating under steam conditions (Pusch et al., 2003). SEM images of laboratory heated bentonite revealed possible opal nodules precipitated at the montmorillonite edges (Figure 1F) and dissolution features on clinoptilolite (Figure 1C, 1D). However, montmorillonite and feldspar fractions remained relatively unchanged (Caporuscio et al., 2013). No montmorillonite illitization was observed for the tested experimental conditions.

Results from XRD analysis of purified FEBEX bentonite showed a mixed layer illite-smectite in all samples, with a low fraction of interstratified illite (SI, Figure S3-S4). Samples dried at room temperature display a (001) distance at 12.0, 11.7, and 11.9 Å, which are expanded to 16.8, 16.3, and 16.7 Å upon glycolation and collapsed to 9.43, 9.51, and 9.51 Å after heating to 450°C for clay samples from the 95°C heater-zone, 50°C heater-zone, and 20°C cold-zone, respectively. Purified FEBEX clay samples from the 95°C heater-zone and cold-zone showed ~5% illite layers, which is slightly lower than the 11% reported for the original bentonite (Fernández et al., 2004), while the purified 50°C heater-zone sample showed ~10% illite layers. These values of 5-10% illite layers are likely within the range of natural variation in bentonite composition and analytical error and therefore, we do not believe that significant illitization has occurred as a result of the 18-year heating of these samples. Similar results have been observed by other

363 researchers for FEBEX samples, with no clear evidence of smectite illitization or changes in bulk
364 mineralogy as a function of radial distance from the heater (Villar et al., 2017).

365 Cation exchange capacity (CEC) was 0.99 ± 0.02, 0.90 ± 0.05, and 0.89 ± 0.02 $mmol_c/g$ for the
366 purified FEBEX 95°C heated-zone, 50°C heated-zone, and 20°C cold-zone samples,
367 respectively. Villar et al. (2017) observed CEC values of 0.88-1.08 $mmol_c/g$ on bulk FEBEX
368 bentonite, with no clear trend with respect to distance from the heater. Therefore, the observed
369 differences in CEC are likely due to sample heterogeneity in the original bentonite blocks rather
370 than a heat-alteration effect. CEC was also measured on the bulk laboratory heated and unheated
371 samples, resulting in values of 0.70 ± 0.01 and 0.69 ± 0.01, respectively. The lower CEC values
372 for the lab-heated bentonite samples reflect the fact that, unlike the FEBEX samples, the lab-
373 heated samples were not purified to remove non-clay impurities which make up approximately
374 28% of the bentonite.

375

376 **Table 4.** Bulk mineralogical composition (weight %) from XRD analysis of laboratory heated
377 and control (initial) bentonite.

	Initial (control) bentonite	Lab-heated bentonite
Montmorillonite	72	71
Quartz	1	3
Cristobalite/Opal-C	2	10
Clinoptilolite	13	4
Analcime	BDL[a]	1
Feldspar	9	10
Biotite	3	<0.5[b]

Pyrite	<0.5[b]	<0.5[b]

[a] BDL = below detection limit

[b] Detected, but below quantification limit of 0.5%

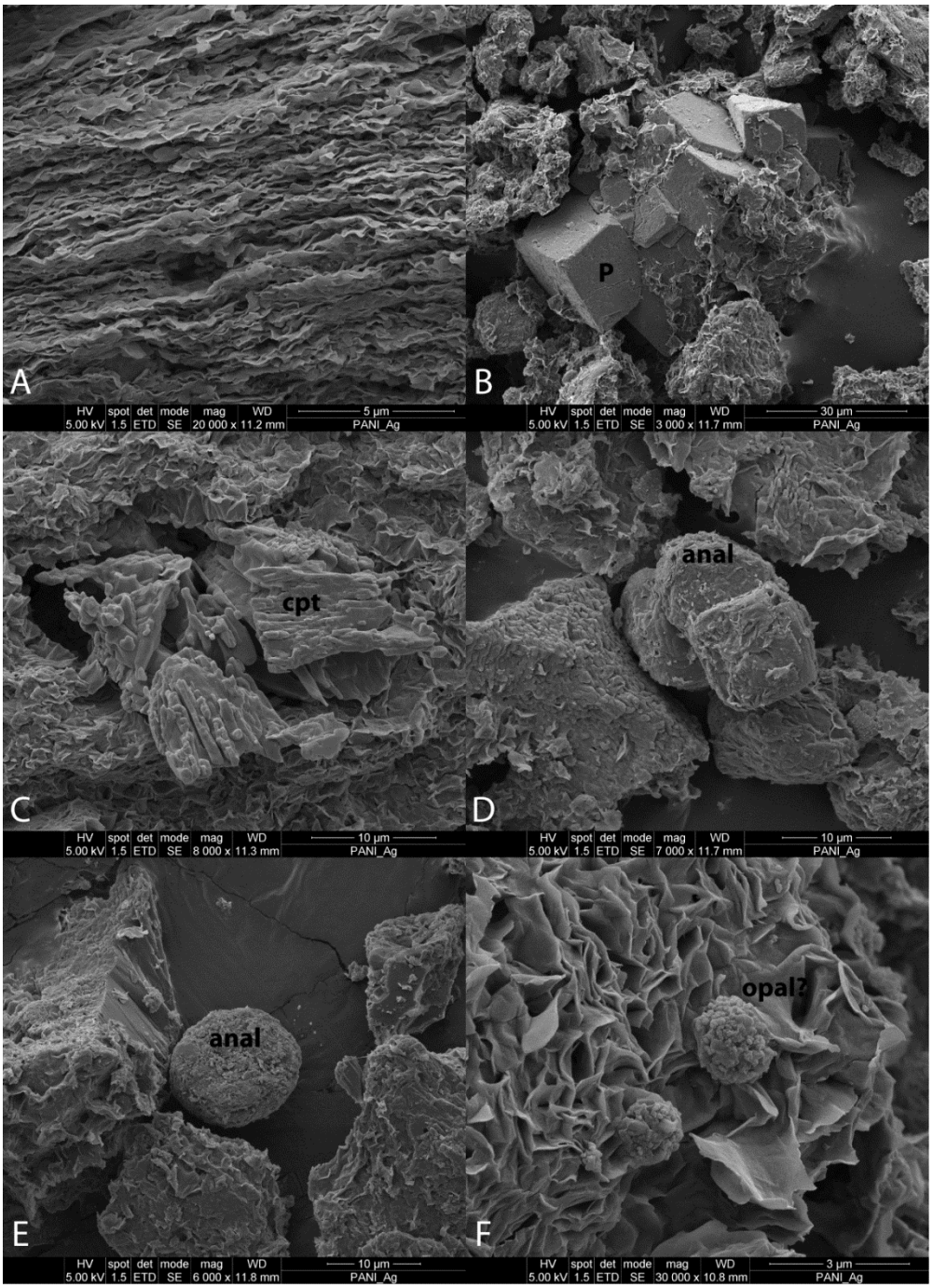

Figure 1. SEM images of lab-heated bentonite. A) Bedding associated with the montmorillonite foils developed during pressurization in a fluid poor environment. B) Unaltered, cubic pyrite. C) Partially altered clinoptilolite showing dissolution features. D) Poorly formed analcime aggregates next to a partially altered clinoptilolite (lower left). E) Deformed analcime particle. F) Possible opaline nodule precipitated on montmorillonite edges.

3.2 Comparison of Uranium(VI) Adsorption on Heated and Unheated Bentonite

Results from U(VI) adsorption experiments onto bulk FEBEX bentonite and bulk lab-heated and control bentonite are shown in Figure 2A and 2B, respectively. U(VI) adsorption onto all bentonite samples showed typical behavior for U(VI) adsorption onto smectite in the presence of atmospheric CO_2, with peak adsorption occurring at circumneutral pH (6-7) (Hyun et al., 2001; Marques Fernandes et al., 2012; Pabalan and Turner, 1996; Tournassat et al., 2018). U(VI) adsorption was lower in the presence of high Ca (~2 mM) compared to low Ca (~0.1 mM), concentrations, especially above pH 7.2, an effect observed for U(VI) adsorption onto many minerals due to the formation of non-sorbing calcium-uranyl-carbonato complexes (Fox et al., 2006; Stewart et al., 2010; Tournassat et al., 2018).

U(VI) adsorption onto unpurified (bulk) FEBEX bentonite was higher for the cold-zone (20°C) compared to the 95°C heated sample over the entire pH range and at both low and high Ca concentrations. Similarly, U(VI) adsorption onto lab-heated bulk bentonite was lower than onto control (unheated) bentonite over the pH range of 4.5-8. Above pH 8, the analytical error is too high due to low U(VI) adsorption to distinguish between the heated and control samples. Below pH 4.5, the lab-heated bentonite displays unusual adsorption behavior. This may be due to

differences in the Ca, Mg, and DIC concentrations (Figure 5) and/or may be the result of U(VI) cation exchange at the lowest pH values.

There are several possible explanations for the lower observed U(VI) adsorption onto heated bentonite: (1) the presence of a lower weight fraction of montmorillonite in heated bentonite, (2) changes in the accessory mineral fraction due to heating, (3) differences in aqueous U(VI) speciation in heated and control/cold-zone bentonite, and (4) changes to the montmorillonite structure or composition with heating. FEBEX bentonite samples were purified to remove accessory minerals, including carbonate minerals, and to isolate the <2 μm clay fraction. Uranium(VI) adsorption experiments were then repeated with purified samples in order to determine if lower observed U(VI) adsorption for the heated sample can be attributed to changes in the clay mineral fraction or other factors. Overall, we see the same trends for heat effects on U(VI) adsorption for bulk and purified bentonite samples. Uranium(VI) adsorption onto purified bentonite was lower on the 95°C heated sample compared to the cold-zone sample over the entire pH range for low Ca experiments (0.1 mM) and at pH 6.8-7.3 for high Ca (2 mM). This suggests that the difference in U(VI) adsorption between 95°C heated and cold zone samples is primarily due to an alteration of the smectite (montmorillonite) clay mineral, and not to differences in pore water chemistry or the types and relative masses of accessory minerals. Uranium(VI) adsorption onto the purified intermediate-heated FEBEX sample (50°C, 75-cm from axis) was similar to the cold-zone sample at 0.1 mM Ca and slightly higher than the cold-zone sample at 2 mM Ca, suggesting that this temperature did not provide sufficient heat for clay alterations.

In all cases, U(VI) adsorption was higher on purified compared to unpurified bentonite. This is expected, because all experiments were performed at the same total solid concentration of 0.5

g/L. Hence, in unpurified bentonite we observe a 'dilution' effect, where clay minerals with a high binding capacity are diluted with accessory minerals (*e.g.*, silica and feldspar) that have a much lower adsorption capacity.

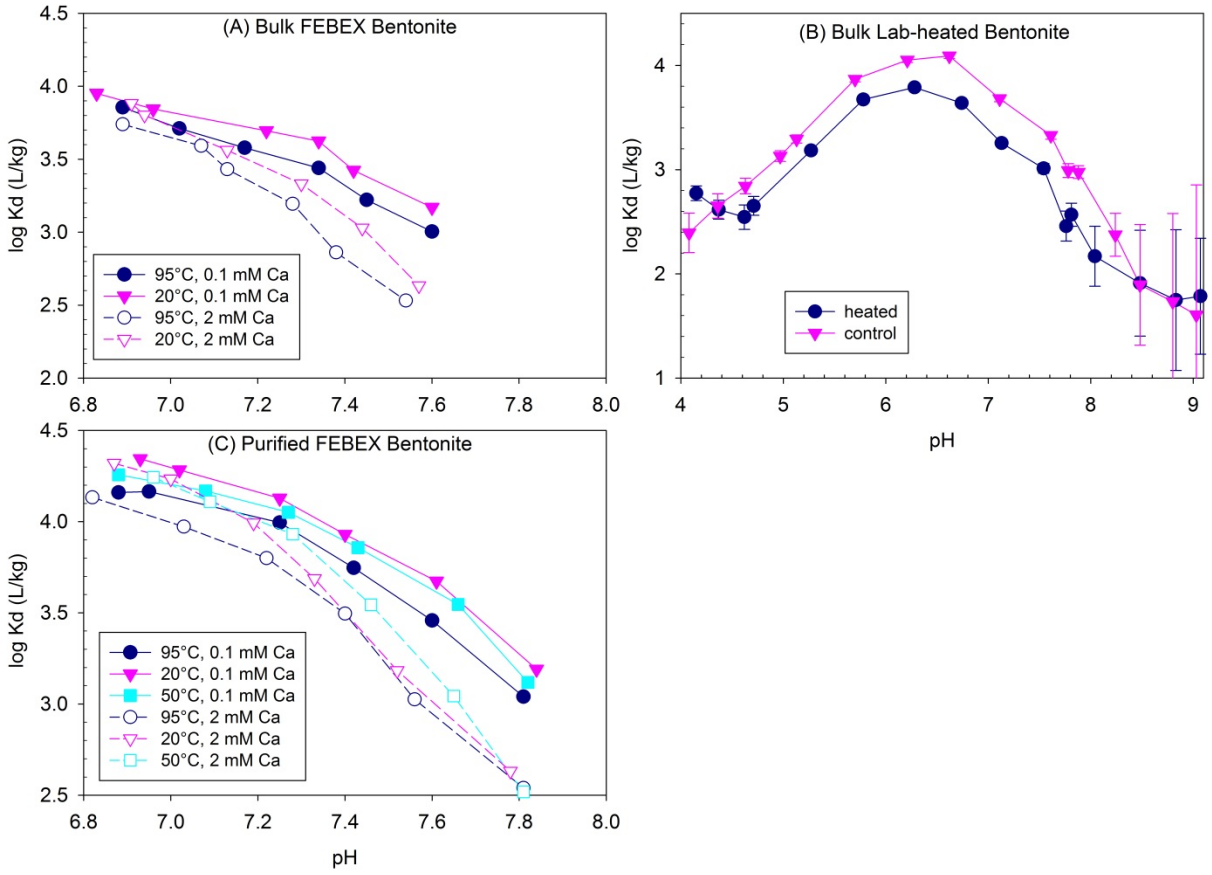

Figure 2. U(VI) adsorption as a function of pH onto (A) bulk FEBEX bentonite, (B) bulk lab-heated and control bentonite, and (C) purified FEBEX bentonite. FEBEX bentonite samples are from the heated-zone (95°C and 50°C) and cold-zone (20°C) and were conducted at two different Ca concentrations. Background Ca concentrations were 0.05-0.08 mM in lab-heated and control bentonite experiments (B). When not visible, error bars, representing analytical error, are smaller than symbols.

3.3 U(VI) Aqueous Speciation

Concentrations of Ca, Mg, and DIC were measured for each set of experimental conditions, and the results are shown along with calculated partial pressure of CO_2 in Figures 3-5. Some small differences in concentrations of Ca, Mg, and DIC were observed between the FEBEX samples, particularly in the 2 mM Ca experiments. Differences in aqueous chemistry between lab-heated and control bentonite were slightly larger compared to the FEBEX samples. These measured concentrations were used, along with assumed concentrations of 0.1 M Na and Cl, for aqueous U(VI) speciation calculations, and detailed results are shown in Figures 6 and 7. Ternary calcium-uranyl-carbonato complexes [$Ca_2UO_2(CO_3)_3(aq)$, $CaUO_2(CO_3)_3^{2-}$] dominate U(VI) aqueous speciation in the presence of 2 mM Ca at pH >7.4 (Figure 6B and 6D). At lower Ca concentrations (0.05-0.1 mM), $CaUO_2(CO_3)_3^{2-}$ species are still very important at pH >7.4, but the $Ca_2UO_2(CO_3)_3(aq)$ species is much lower in concentration (Figure 6A and 6C). Uranyl-carbonato complexes are important at circum-neutral to alkaline pH (~5.5-9), particularly at the lower Ca concentrations (0.05-0.1 mM) for both the laboratory-heated (Figure 7) and FEBEX bentonite experiments. Aqueous U(VI) speciation is similar, but not identical, for purified and bulk FEBEX bentonite samples, with the primary difference being the formation of the magnesium-uranyl-carbonato complex [$MgUO_2(CO_3)_3^{-2}$] in the bulk samples. This results from the small amount of Mg found in the porewater of unpurified bentonite.

According to Tournassat et al. (2018), uranyl-carbonato surface complexes do not necessarily have to be included to simulate U(VI) sorption to montmorillonite over a range of aqueous chemical conditions (pH, DIC, and Ca concentrations). The authors developed a surface complexation model that specifically accounts for the so-called spillover effect, the influence of the electrostatic potential of basal surface sites on the electrostatic potential of surface complexation sites on clay edges. This model accurately describes U(VI) adsorption to

montmorillonite with only one U(VI) adsorption site and three surface complexes: $>SiteH_3UO_2^{+2}$, $>SiteHUO_2$, and $>SiteUO_2(OH)_2^{-3}$ (Tournassat et al., 2018). Based on this model, only the uranyl cation (UO_2^{+2}) and uranyl hydroxyl species [$UO_2(OH)^+$, $UO_2(OH)_2$, and $UO_2(OH)_3^-$] participate in adsorption, while uranyl-carbonato and calcium-uranyl-carbonato species do not adsorb.

We have calculated the sum of aqueous uranyl and uranyl hydroxyl species for each experiment (Figure 8) in order to aid in the interpretation of the effect of U(VI) aqueous speciation on adsorption during the experiments. Several observations can be made based on these calculations. First, uranyl-hydroxyl species concentrations are nearly identical across all FEBEX samples and Ca concentrations at pH 6.8-7.2, while at pH >7.3 uranyl-hydroxyl concentrations are higher in the presence of 0.1 mM Ca compared to 2 mM Ca. These observations are consistent with U(VI) sorption data (Figure 2) which show a divergence in the U(VI) adsorption as a function of Ca concentration around pH 7.3. This provides further evidence that changes in aqueous U(VI) speciation are the cause of differences in U(VI) adsorption between the two Ca concentrations. Second, uranyl-hydroxyl concentrations are slightly lower for bulk FEBEX samples compared to purified FEBEX samples at pH >7.3. While this difference in uranyl-hydroxyl concentrations is small, it may be due to the formation of the magnesium-uranyl-carbonato complex in bulk samples. Third, differences in uranyl-hydroxyl concentrations for the heated and cold-zone FEBEX samples are generally minor or non-existent. In the presence of 2 mM Ca, there is a slightly higher concentration of uranyl-hydroxyl species for the heated purified FEBEX samples (95°C and 50°C) compared to the cold-zone purified samples above pH 7.2 (Figure 8C). This observation may explain why we do not observe lower U(VI) sorption onto the heated sample for these data points. In other words, the lower U(VI)

sorption onto heated bentonite (which is observed at all other conditions) is masked by slight differences in aqueous speciation for these experimental data points. A similar effect was observed for the intermediate-heated (50°C) sample, with slightly higher concentrations of uranyl-hydroxyl species and corresponding higher U(VI) adsorption at pH > 7.2. These observations provide strong pieces of evidence that the observed lower U(VI) adsorption onto heated FEBEX bentonite must be due to structural differences in clay minerals, and not to differences in aqueous U(VI) speciation.

For the lab-heated bentonite experiments, differences in aqueous U(VI) speciation between heated and control bentonite are significant over the pH range 5.8-8.5 (Figure 8). The lower uranyl-hydroxyl concentrations for heated bentonite compared to control bentonite is due to higher observed DIC concentrations for the same pH values in heated samples (Figure 5), which leads to higher calculated CO_2 concentrations (up to 2,094 ppm) and a larger fraction of uranyl-carbonato complexes. It is unlikely that this difference in U(VI) speciation between the lab heated and control samples is sufficient to explain all of the observed difference in U(VI) adsorption. For example, the concentrations of uranyl-hydroxyl species are nearly identical below pH 5.8 for these samples, while a difference in U(VI) adsorption is still observed. Hence, it is likely that the observed changes in U(VI) adsorption are due to a combination of different aqueous U(VI) speciation and changes in clay and/or accessory minerals. Results from aqueous speciation calculations emphasize the importance of accurate pH, DIC, and Ca measurements for the interpretation of U(VI) adsorption data and predictions of U(VI) mobility in waste disposal scenarios, a conclusion also reached by Tournassat et al. (2018).

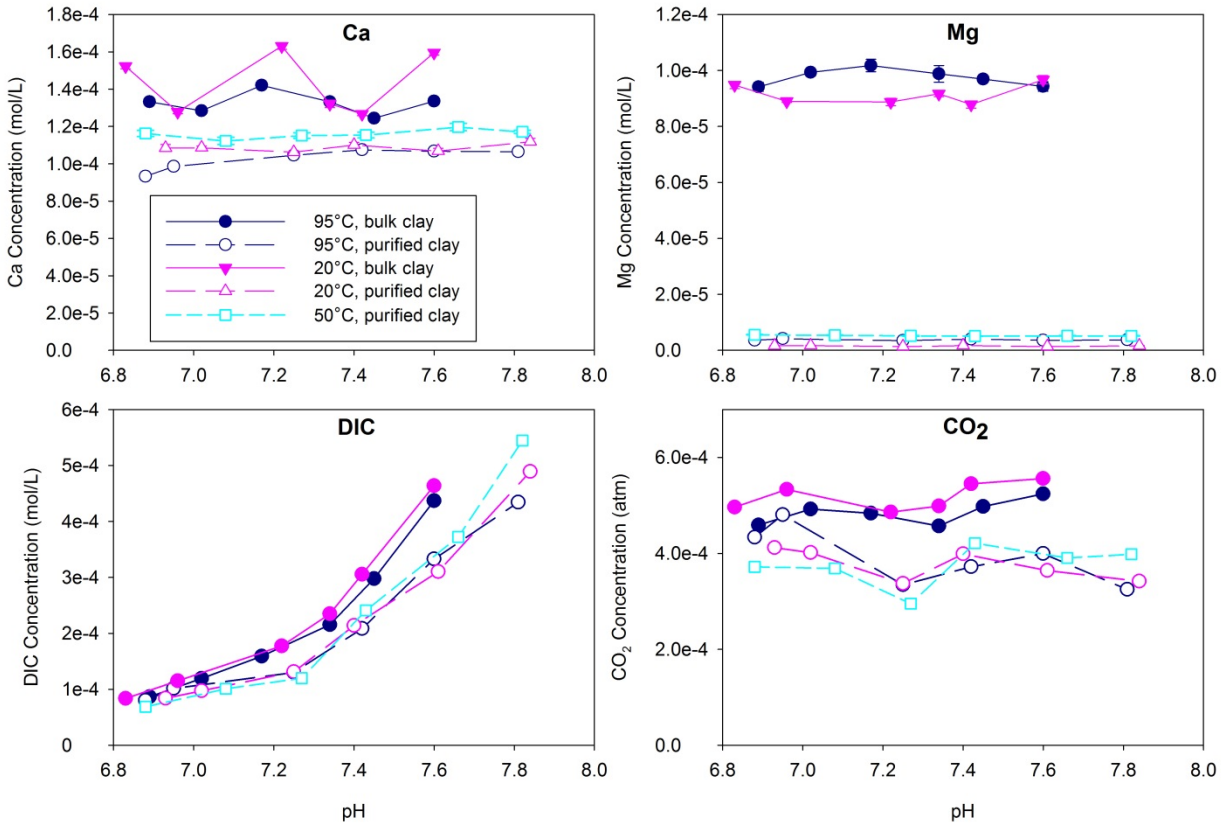

Figure 3. Measured concentrations of dissolved Ca, Mg, and DIC along with calculated partial pressure of CO_2 are shown for U(VI) adsorption experiments conducted in the presence of low Ca (0.1 mM) on FEBEX heated (50°C and 95°C) and cold-zone (20°C) bentonite. Data is shown for both bulk and purified clays. Error bars representing analytical error are smaller than symbols.

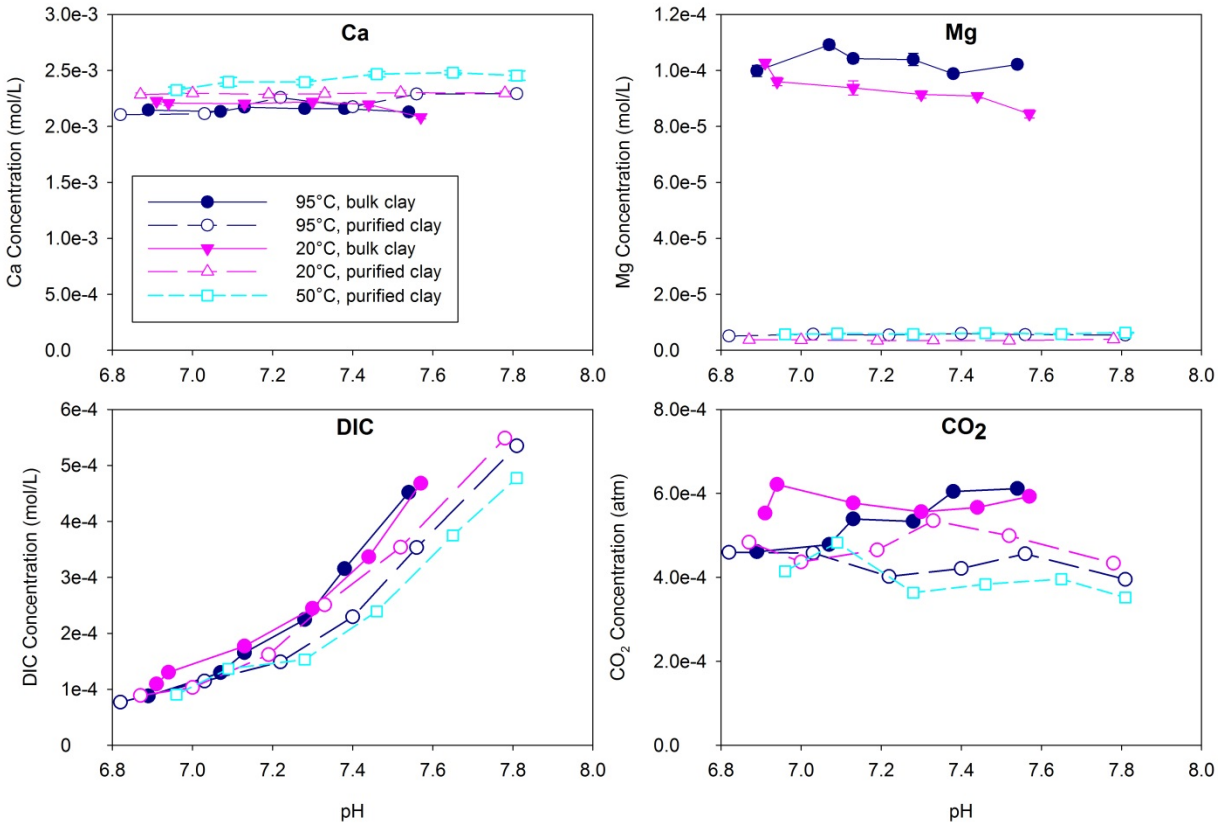

Figure 4. Measured concentrations of dissolved Ca, Mg, and DIC along with calculated partial pressure of CO_2 are shown for U(VI) adsorption experiments conducted in the presence of high Ca (2 mM) on FEBEX heated (50°C and 95°C) and cold-zone (20°C) bentonite. Data is shown for both bulk and purified clays. Error bars representing analytical error are smaller than symbols.

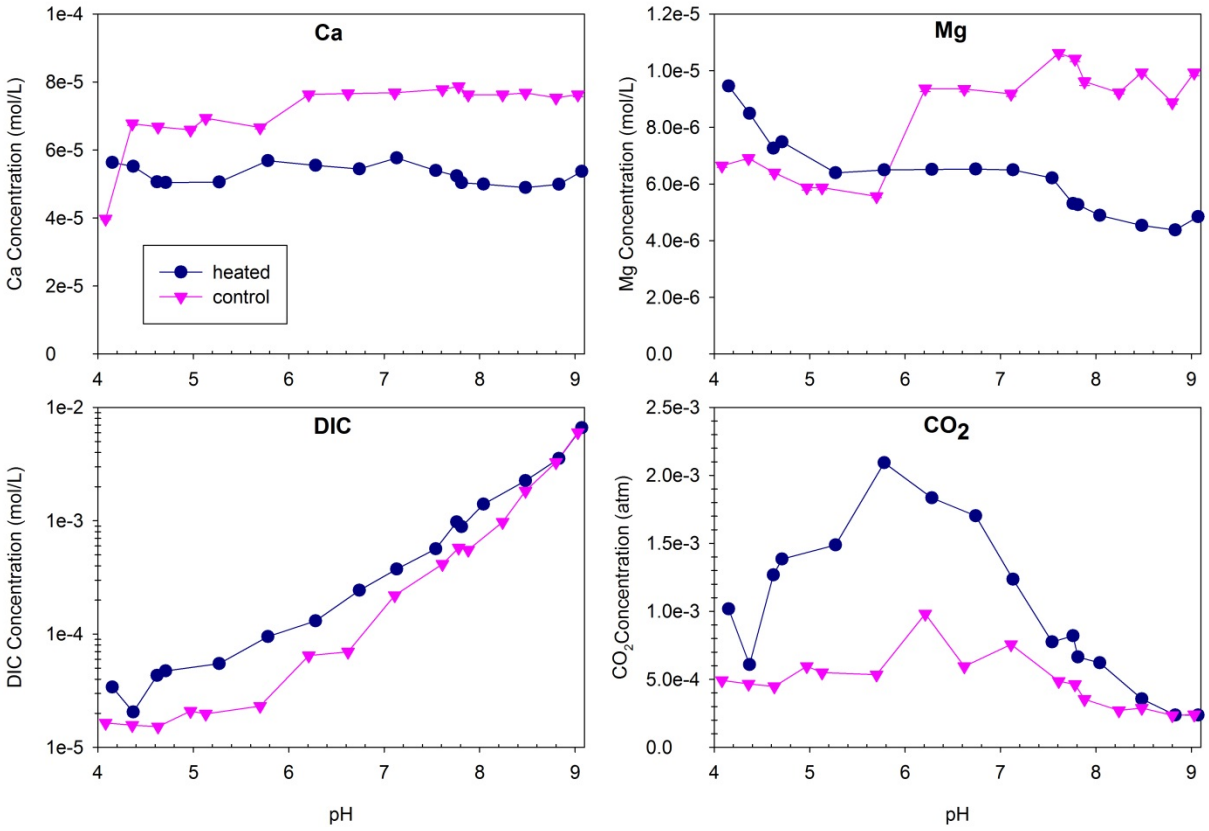

516

517 **Figure 5.** Measured concentrations of dissolved Ca, Mg, and DIC along with calculated partial

518 pressure of CO_2 are shown for U(VI) adsorption experiments on laboratory heated and control

519 bentonite. Error bars representing analytical error are smaller than symbols.

520

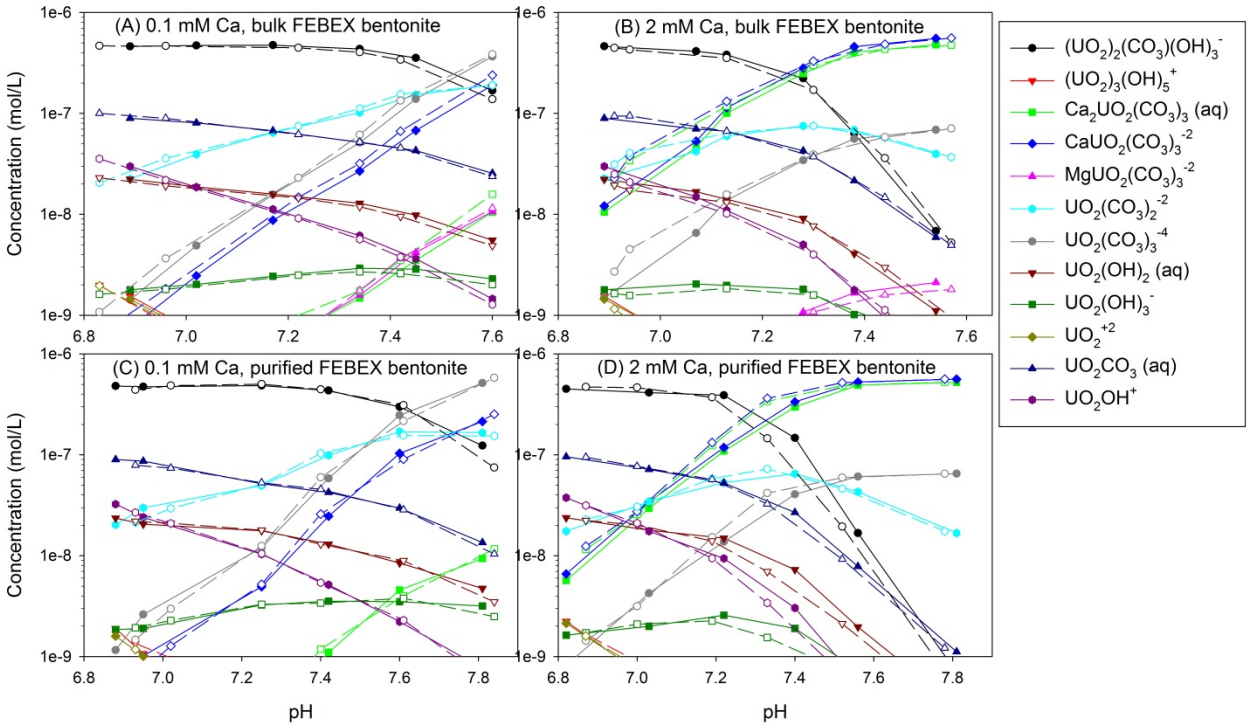

521

522 **Figure 6.** Aqueous U(VI) speciation calculated for U(VI) adsorption experiments with FEBEX
523 bentonite. (A) bulk FEBEX bentonite with 0.1 mM Ca, (B) bulk FEBEX bentonite with 2 mM
524 Ca, (C) purified FEBEX bentonite with 0.1 mM Ca, and (D) purified FEBEX bentonite with 2
525 mM Ca. Solid lines with filled symbols represent 95°C-heated bentonite and dashed lines with
526 open symbols represent 20°C cold-zone bentonite.

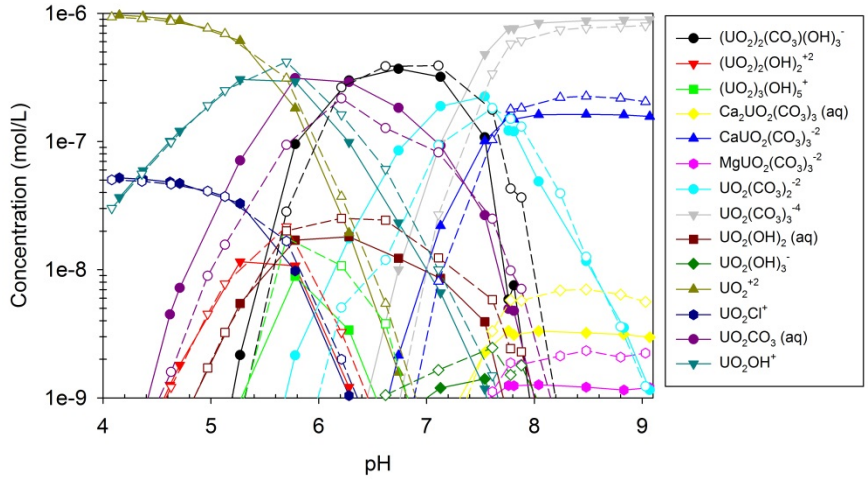

527

Figure 7. Aqueous U(VI) speciation calculated for U(VI) adsorption experiments with lab-heated (solid lines with filled symbols) and control (dashed lines with open symbols) bentonite.

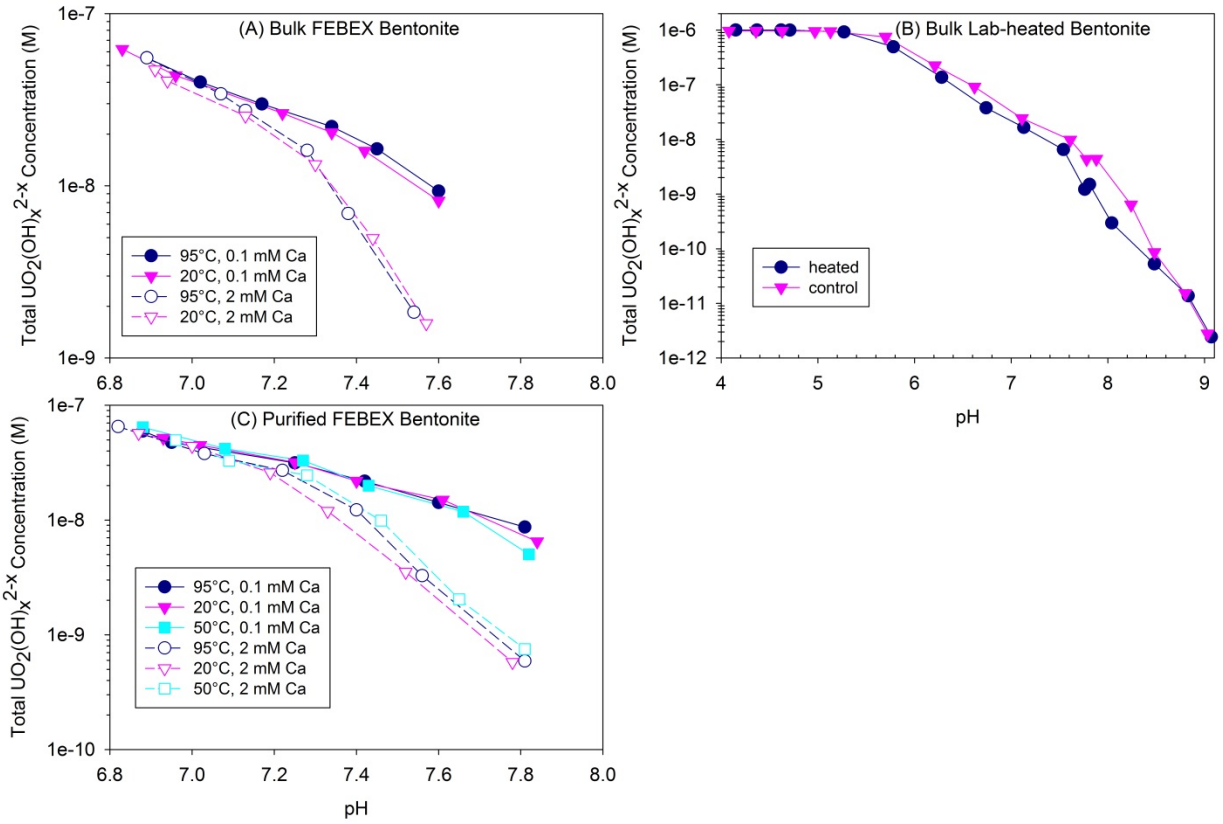

Figure 8. Sum of uranyl hydroxyl aqueous species $[UO_2(OH)_x^{2-x}$, where x varies between 0 and 3] during experiments on (A) bulk FEBEX bentonite, (B) bulk lab-heated and control bentonite, and (C) purified FEBEX bentonite as a function of pH.

3.4 Potential Heat-Induced Changes to Clay Minerals

Our observations of lower U(VI) adsorption onto heated bentonite over a range of chemical conditions suggests that heat-induced changes have occurred to montmorillonite. However, no evidence of illitization was observed in either the lab-heated or field-heated (FEBEX) samples. A slightly higher CEC was measured for the heated FEBEX bentonite compared to cold-zone

bentonite (purified clay samples). However, this difference in CEC is unlikely to cause lower U(VI) adsorption under the conditions investigated in this study. Under neutral to alkaline pH conditions, U(VI) is known to adsorb to edge sites of montmorillonite forming inner-sphere bidentate complexes (Hennig et al., 2002; Marques Fernandes et al., 2012; Schlegel and Descostes, 2009; Tournassat et al., 2018; Zhang et al., 2018). Cation exchange of U(VI) is only important under low pH and low ionic strength conditions (Tournassat et al., 2018). Therefore, small differences in the characteristics of montmorillonite edge sites may have a relatively large effect on U(VI) adsorption. Specifically, the (1) relative proportion of AC and B type edge sites, as described by White and Zelazny (1988), (2) total edge surface area, and (3) electrostatic properties of the basal surface which influences the electrostatic potential of edge sites through the spillover effect as described in the literature (Tournassat et al., 2016; Tournassat et al., 2018; Zhang et al., 2018) will control U(VI) adsorption to montmorillonite. These changes are difficult, if not impossible, to accurately and quantitatively characterize experimentally, but may have a significant impact on the adsorption capacity of the mineral. SEM images of lab-heated bentonite revealed the formation of opal nodules at the edges of montmorillonite and XRD results showed an increase in the opal fraction from 2 to 10% after heating. These nodules may block the edge adsorption sites, and therefore may be at least partially responsible for the lower U(VI) adsorption observed on heated bentonite. Other radionuclides that also adsorb to edge sites of clay minerals may be similarly affected.

3.5 Implications for Radioactive Waste Disposal

Temperatures in high level radioactive waste repositories may reach values as high as 100-300°C, depending on the waste disposal scenario (Hardin et al., 2013; Horseman and McEwen, 1996). Our results show that after 18 years of heating at a maximum temperature of 100°C,

U(VI) adsorption is affected only in samples closest to the heater (*i.e.*, within 25-cm) which experienced the highest temperatures (95°C). The heat-induced decrease in U(VI) adsorption corresponds to an average 31% decrease in K_d values (or ~0.2 log K_d units). No apparent changes in U(VI) adsorption were observed at further distances from the heater which experienced lower temperatures (35-50°C). Interestingly, lab-scale heating experiments conducted at a much higher temperature (300°C) but over a shorter time-frame (7 weeks) lead to very similar conclusions with regard to a decrease in U(VI) sorption due to bentonite exposure to heat, although the extent of heat-induced changes was slightly larger. Here, K_d values decreased by an average of 50% for bentonite after lab-heating at 300°C. This suggests that the use of lab-scale heating experiments may be a relatively fast, cost-effective tool to support the selection of experimental conditions to be tested on the field scale. At this point, it is unknown whether heating at even higher temperatures (*e.g.*, 200°C) and over longer time periods (100 years) under field conditions would continue this trend of lowering U(VI) adsorption; hence, this topic warrants further research. High levels of salts, particularly Ca and Mg, which may be found near waste canisters after groundwater intrusion into the engineered clay barrier and subsequent evaporation (Villar et al., 2017), can further decrease U(VI) adsorption onto clay due to changes in aqueous U(VI) speciation and ionic strength. However, lower pH and DIC concentrations were observed in both lab-heated and field-heated bentonite, which may counter the effects of high ionic strength and Ca concentration on U(VI) adsorption.

The decreased adsorption observed in this study as a result of bentonite heating may impact the diffusion of U(VI) through engineered clay barriers and must be considered when designing and assessing radioactive waste repositories. A 30-50% decrease in K_d will have a large impact on the transport behavior of U(VI) in clay media in waste disposal scenarios due to the much higher

586 degree of compaction (*i.e.*, solid concentration) present in engineered barriers (*e.g.*, 1650 kg/m^3)
587 and natural clay rocks.

588 We performed diffusion calculations in order to demonstrate the potential impacts of heat-
589 induced alterations on U(VI) diffusion through an engineered barrier. Uranium(VI) diffusion
590 profiles in bulk FEBEX bentonite were calculated after 20,000 and 100,000 years of U(VI)
591 leaking from a constant concentration source as described in section 2.7 and using K_d values
592 from experiments on bulk FEBEX bentonite (Table 5). In the presence of 0.1 mM Ca, the
593 observed differences in U(VI) K_d values between 95°C heated and cold-zone bentonite can result
594 in greater transport distances in heated bentonite compared to cold-zone bentonite. Similarly,
595 U(VI) transport is greater in the presence of 2 mM Ca compared to 0.1 mM Ca.

596 While these diffusion calculations represent a simplistic waste disposal scenario which doesn't
597 take into account changes in porewater chemistry or the source term over time, they provide a
598 first estimate of the magnitude of changes in U(VI) porewater concentrations that can be
599 expected as a result of heat-induced alterations in the bentonite barrier. The ultimate effect of
600 these heat-induced alterations on U(VI) mobility will depend on the specific time, location and
601 chemical solution conditions present in the clay. Performance assessments should account for at
602 least a 30-50% decrease in K_d values that were measured for the original clay material as a result
603 of heating.

604

605 **Table 5.** U(VI) K_d values for bulk FEBEX bentonite used for diffusion estimates.

Bentonite	**[Ca] (mM)**	**pH**	**K_d (L/kg)**
20°C cold-zone	0.1	7.60	1011

95°C heated-zone	0.1	7.60	1481
20°C cold-zone	2.0	7.57	430
95°C heated-zone	2.0	7.54	340

606

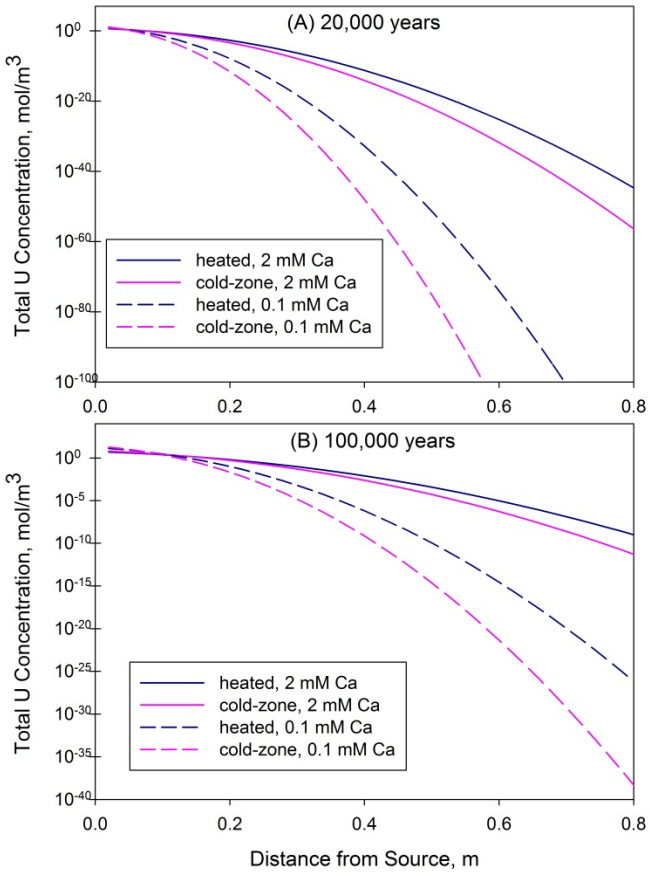

607

608 **Figure 9.** Estimated U(VI) diffusion profiles in compacted FEBEX bentonite as a function of Ca
609 concentration (0.1 or 2 mM Ca) and heat-exposure (bulk cold-zone bentonite and 95°C heated
610 bentonite) after 20,000 (A) and 100,000 years (B). Total U(VI) concentration includes adsorbed
611 and dissolved U(VI) expressed in terms of total bentonite volume (m^3). Diffusion calculations
612 were based on diffusion parameters listed in Table 2 and U(VI) K_d values listed in Table 5.

613

Acknowledgements

The authors wish to thank Dr. Christophe Tournassat (BRGM), Dr. James A. Davis (LBNL), and Dr. Liange Zheng (LBNL) for helpful discussions. Dr. Liange Zheng (LBNL) provided the FEBEX bentonite samples. Two anonymous reviewers and Dr. Gimmi provided helpful comments that improved the manuscript. P.M.F., P.S.N., and R.M.T. were funded by the Spent Fuel and Waste Science and Technology Program, Office of Nuclear Energy of the US Department of Energy under contract number DE-AC02-05CH11231 with Lawrence Berkeley National Laboratory. R.M.T. was additionally supported by the DOE Office of Nuclear Energy through the Nuclear Energy University Program (Federal Grant Number: DE-NE0008683). M.C.C. was funded through the U.S. Department of Energy, Office of Science, Office of Basic Energy Sciences, Chemical Sciences, Geosciences, and Biosciences Division during the completion of the manuscript. M.C.C. and F.C. were supported by the Department of Energy's Used Fuel Disposition campaign during sample preparation.

Supporting Information

Supporting information (SI) can be downloaded free of charge online. The SI includes detailed mineralogical characterization (XRD), detailed bentonite purification methods, and U(VI) adsorption kinetics on FEBEX bentonite samples.

Data Availability

Data used in this manuscript is available free of charge on Mendeley Data, online at https://data.mendeley.com/

References

Altmann, S., 2008. 'Geo'chemical research: A key building block for nuclear waste disposal safety cases. J. Contam. Hydrol. 102, 174-179.

637 Altmann, S., Tournassat, C., Goutelard, F., Parneix, J.-C., Gimmi, T., Maes, N., 2012. Diffusion-
638 driven transport in clayrock formations. Appl. Geochem. 27, 463-478.
639 Bradbury, M.H., Baeyens, B., 2005. Modelling the sorption of Mn(II), Co(II), Ni(II), Zn(II),
640 Cd(II), Eu(III), Am(III), Sn(IV), Th(IV), Np(V) and U(VI) on montmorillonite: Linear free
641 energy relationships and estimates of surface binding constants for some selected heavy metals
642 and actinides. Geochim. Cosmochim. Acta 69, 875-892.
643 Caporuscio, F., Cheshire, M., Rearick, M., Jove-Colon, C., 2014. LANL Argillite EBS
644 Experimental Program 2014. DOE Report No. FCRD-UFD-2014-000491, U.S. Department of
645 Energy (DOE).
646 Caporuscio, F.A., Chesire, M.C., Rearick, M.S., McCarney, M.K., Jove-Colon, C., 2013. EBS
647 Report-LANL Experimental update of buffer/backfill at elevated P, T. DOE Report No. FCRD-
648 UFD-2013-000207, Los Alamos National Laboratory, Los Alamos, NM (United States).
649 Cheshire, M.C., Caporuscio, F.A., Rearick, M.S., Jové-Colón, C., McCarney, M.K., 2014.
650 Bentonite evolution at elevated pressures and temperatures: An experimental study for generic
651 nuclear repository designs. Amer. Mineralogist 99, 1662-1675. DOI: 10.2138/am.2014.4673
652 Chung, F.H., 1974. Quantitative interpretation of X-ray diffraction patterns of mixtures. I.
653 Matrix-flushing method for quantitative multicomponent analysis. J. Appl. Crystallography 7,
654 519-525. DOI: 10.1107/S0021889874010375
655 Couture, R.A., 1985. Steam rapidly reduces the swelling capacity of bentonite. Nature 318, 50-
656 52.
657 Cuadros, J., Linares, J., 1996. Experimental kinetic study of the smectite-to-illite transformation.
658 Geochim. Cosmochim. Acta 60, 439-453. DOI: 10.1016/0016-7037(95)00407-6

Delay, J., Vinsot, A., Krieguer, J.-M., Rebours, H., Armand, G., 2007. Making of the underground scientific experimental programme at the Meuse/Haute-Marne underground research laboratory, North Eastern France. Phys.Chem.Earth, Parts A/B/C 32, 2-18. DOI: 10.1016/j.pce.2006.04.033

Detzner, K., Kober, F., 2015. FEBEX-DP drilling and sampling report sections 32-34, Internal Report. AN15-714, NAGRA.

Dong, W., Brooks, S.C., 2006. Determination of the Formation Constants of Ternary Complexes of Uranyl and Carbonate with Alkaline Earth Metals (Mg^{2+}, Ca^{2+}, Sr^{2+}, and Ba^{2+}) Using Anion Exchange Method. Environ. Sci. Technol. 40, 4689-4695. DOI: 10.1021/es0606327

Drits, V.A., Varaxina, T.V., Sakharov, B.A., Plancon, A., 1994. A simple technique for identification of one-dimensional powder X-ray diffraction patterns for mixed-layer illite-smectites and other interstratified minerals. Clays Clay Minerals 42, 382-390. DOI: 10.1346/CCMN.1994.0420402

Eberl, D., Velde, B., McCormick, T., 1993. Synthesis of illite-smectite from smectite at earth surface temperatures and high pH. Clay Minerals 28, 49-49. DOI:10.1180/claymin.1993.028.1.06

ENRESA, 2000. FEBEX Project: Full-scale engineered barriers experiment for a deep geological repository for high level radioactive waste in crystalline host rock. Final Report. Tech Publ. 01/2000 ENRESA.

Fernández, A.M., Baeyens, B., Bradbury, M., Rivas, P., 2004. Analysis of the porewater chemical composition of a Spanish compacted bentonite used in an engineered barrier. Phys.Chem.Earth, Parts A/B/C 29, 105-118. DOI: 10.1016/j.pce.2003.12.001

Fox, P.M., Davis, J.A., Hay, M.B., Conrad, M.E., Campbell, K.M., Williams, K.H., Long, P.E., 2012. Rate-limited U(VI) desorption during a small-scale tracer test in a heterogeneous uranium-contaminated aquifer. Water Resour. Res. 48, W05512. DOI: 10.1029/2011wr011472

Fox, P.M., Davis, J.A., Zachara, J.M., 2006. The effect of calcium on aqueous uranium(VI) speciation and adsorption to ferrihydrite and quartz. Geochim. Cosmochim. Acta 70, 1379-1387. DOI: 10.1016/j.gca.2005.11.027

García-Gutiérrez, M., Cormenzana, J.L., Missana, T., Mingarro, M., Alonso, U., 2003. Analysis of Uranium Diffusion Coefficients in Compacted FEBEX Bentonite. MRS Proc. 807, 603. DOI: 10.1557/proc-807-603

Giffaut, E., Grivé, M., Blanc, P., Vieillard, P., Colàs, E., Gailhanou, H., Gaboreau, S., Marty, N., Madé, B., Duro, L., 2014. Andra thermodynamic database for performance assessment: ThermoChimie. Appl.Geochem. 49, 225-236. DOI: 10.1016/j.apgeochem.2014.05.007

Guillaumont, R., Fanghanel, T., Neck, V., Fuger, J., Palmer, D.A., Grenthe, I., Rand, M.H., 2003. Update on the chemical thermodynamics of uranium, neptunium, plutonium, americium, and technetium. Elsevier, Amsterdam.

Guyonnet, D., Touze-Foltz, N., Norotte, V., Pothier, C., Didier, G., Gailhanou, H., Blanc, P., Warmont, F., 2009. Performance-based indicators for controlling geosynthetic clay liners in landfill applications. Geotextiles and Geomembranes 27, 321-331. DOI: 10.1016/j.geotexmem.2009.02.002

Hadi, J., Tournassat, C., Ignatiadis, I., Greneche, J.M., Charlet, L., 2013. Modelling CEC variations versus structural iron reduction levels in dioctahedral smectites. Existing approaches, new data and model refinements. J.Colloid Interface Sci. 407, 397-409. DOI: 10.1016/j.jcis.2013.05.014

Hardin, E., Clayton, D., Howard, R., Scaglione, J., Pierce, E., Banerjee, K., Voegele, M., Greenberg, H., Wen, J., Buscheck, T., 2013. Preliminary Report on Dual-Purpose Canister Disposal Alternatives (FY13). DOE Report #: FCRD-UFD-2013-000171, US Department of Energy, Used Fuel Disposition Campaign.

Hennig, C., Reich, T., Dähn, R., Scheidegger, A.M., 2002. Structure of uranium sorption complexes at montmorillonite edge sites, Radiochim. Acta, 90, 653. DOI: 10.1524/ract.2002.90.9-11_2002.653

Horseman, S.T., McEwen, T.J., 1996. Thermal constraints on disposal of heat-emitting waste in argillaceous rocks. Eng. Geol. 41, 5-16. DOI: 10.1016/0013-7952(95)00046-1

Hyun, S.P., Cho, Y.H., Hahn, P.S., Kim, S., 2001. Sorption mechanism of U(VI) on a reference montmorillonite: Binding to the internal and external surfaces. J. Radioanalyt. Nuclear Chem. 250, 55-62. DOI: 10.1023/a:1013212130177

Johnson, L., Niemeyer, M., Klubertanz, G., Siegel, P., Gribi, P., 2002. Calculations of the temperature evolution of a repository for spent fuel, vitrified high-level waste and intermediate level waste in Opalinus Clay. NAGRA Technical Report 01-04. National Cooperative for the Disposal of Radioactive Waste, NAGRA, Switzerland.

Marques Fernandes, M., Baeyens, B., Dähn, R., Scheinost, A.C., Bradbury, M.H., 2012. U(VI) sorption on montmorillonite in the absence and presence of carbonate: A macroscopic and microscopic study. Geochim. Cosmochim. Acta 93, 262-277. DOI: 10.1016/j.gca.2012.04.017

Moore, D.M., Reynolds, R.C., 1989. X-ray Diffraction and the Identification and Analysis of Clay Minerals. Oxford university press Oxford.

Pabalan, R.T., Turner, D.R., 1996. Uranium(6+) sorption on montmorillonite: Experimental and surface complexation modeling study. Aq. Geochem. 2, 203-226. DOI: 10.1007/bf01160043

727 Pusch, R., Bluemling, P., Johnson, L., 2003. Performance of strongly compressed MX-80 pellets
728 under repository-like conditions. Appl. Clay Sci. 23, 239-244. DOI: 10.1016/S0169-
729 1317(03)00108-X
730 Schlegel, M.L., Descostes, M., 2009. Uranium Uptake by Hectorite and Montmorillonite: A
731 Solution Chemistry and Polarized EXAFS Study. Environ. Sci. Technol. 43, 8593-8598. DOI:
732 10.1021/es902001k
733 Shackelford, C.D., 1991. Laboratory diffusion testing for waste disposal — A review. J. Contam.
734 Hydrol. 7, 177-217. DOI: 10.1016/0169-7722(91)90028-Y
735 SKB, 2011. Long-term safety for the final repository for spent nuclear fuel at Forsmark. Main
736 report of the SR-Site project. Report No. SKB-TR-11-01 (V. 3), Swedish Nuclear Fuel and
737 Waste Management Co.
738 Smith, R.M., Martell, A.E., Motekaitis, R.J., 2003. NIST critically selected stability constants of
739 metal complexes database, NIST standard reference database 46, version 7.0. NIST,
740 Gaithersburg, MD, USA.
741 Srodon, J., 1980. Precise identification of illite/smectite interstratifications by X-ray powder
742 diffraction. Clays Clay Miner. 28, 401.
743 Stewart, B.D., Mayes, M.A., Fendorf, S., 2010. Impact of Uranyl−Calcium−Carbonato
744 Complexes on Uranium(VI) Adsorption to Synthetic and Natural Sediments. Environ. Sci.
745 Technol. 44, 928-934. DOI: 10.1021/es902194x
746 Tinnacher, R.M., Holmboe, M., Tournassat, C., Bourg, I.C., Davis, J.A., 2016. Ion adsorption
747 and diffusion in smectite: Molecular, pore, and continuum scale views. Geochim. Cosmochim.
748 Acta 177, 130-149. DOI: 10.1016/j.gca.2015.12.010

749 Tournassat, C., Davis, J.A., Chiaberge, C., Grangeon, S., Bourg, I.C., 2016. Modeling the Acid–
750 Base Properties of Montmorillonite Edge Surfaces. Environ. Sci. Technol. 50, 13436-13445.
751 DOI: 10.1021/acs.est.6b04677
752 Tournassat, C., Steefel, C.I., Bourg, I.C., Bergaya, F., 2015. Natural and engineered clay
753 barriers. Vol. 6. Elsevier.
754 Tournassat, C., Tinnacher, R.M., Grangeon, S., Davis, J.A., 2018. Modeling uranium(VI)
755 adsorption onto montmorillonite under varying carbonate concentrations: A surface
756 complexation model accounting for the spillover effect on surface potential. Geochim.
757 Cosmochim. Acta 220, 291-308. DOI: 10.1016/j.gca.2017.09.049
758 Villar, M.V., Fernández, A.M., Romero, E., Dueck, A., Cuevas, J., Plotze, M., Kaufhold, S.,
759 Dohrmann, R., Iglesias, R.J., Sakaki, T., Voltolini, M., Zheng, L., Dawamoto, K., Kober, F.,
760 2017. FEBEX-DP Post-mortem THM/THG Analysis Report. NAGRA.
761 Villar, M.V., Fernández, A.M., Romero, E., Dueck, A., Cuevas, J., Plotze, M., Kaufhold, S.,
762 Dohrmann, R., Iglesias, R.J., Sakaki, T., Voltolini, M., Zheng, L., Dawamoto, K., Kober, F.,
763 2017. FEBEX-DP Post-mortem THM/THG Analysis Report. Report No. NAB 16-17, NAGRA.
764 Villar, M.V., Iglesias, R.J., García-Siñeriz, J.L., 2018a. State of the in situ Febex test (GTS,
765 Switzerland) after 18 years: a heterogeneous bentonite barrier. Environ. Geotechnics, 1-13. DOI:
766 10.1680/jenge.17.00093
767 Villar, M.V., Iglesias, R.J., Gutiérrez-Álvarez, C., Carbonell, B., 2018b. Hydraulic and
768 mechanical properties of compacted bentonite after 18years in barrier conditions. Appl. Clay Sci.
769 160, 49-57. DOI: 10.1016/j.clay.2017.12.045
770 Wersin, P., Johnson, L.H., McKinley, I.G., 2007. Performance of the bentonite barrier at
771 temperatures beyond 100°C: A critical review. Phys.Chem.Earth, Parts A/B/C 32, 780-788.

772 White, G.N., Zelazny, L.W., 1988. Analysis and implications of the edge structure of
773 dioctahedral phyllosilicates. Clays Clay Minerals 36, 141-146. DOI:
774 10.1346/ccmn.1988.0360207
775 Zhang, C., Liu, X., Tinnacher, R.M., Tournassat, C., 2018. Mechanistic Understanding of Uranyl
776 Ion Complexation on Montmorillonite Edges: A Combined First-Principles Molecular
777 Dynamics–Surface Complexation Modeling Approach. Environ. Sci. Technol. 50, 8501-8509.
778 DOI: 10.1021/acs.est.8b02504
779 Zheng, L., Rutqvist, J., Birkholzer, J.T., Liu, H.-H., 2015. On the impact of temperatures up to
780 200°C in clay repositories with bentonite engineer barrier systems: A study with coupled
781 thermal, hydrological, chemical, and mechanical modeling. Engin. Geol. 197, 278-295. DOI:
782 10.1016/j.enggeo.2015.08.026

783